Research Paper

Mst1 promotes mitochondrial dysfunction and apoptosis in oxidative stress-induced rheumatoid arthritis synoviocytes

Yingjie Wang[1,*], Qi Yang[1,2,*], Songpo Shen[1,3], Linjie Zhang[1], Yongbo Xiang[1], Xisheng Weng[1]

[1]Department of Orthopedic Surgery, Peking Union Medical College Hospital, Peking Union Medical College and Chinese Academy of Medical Science, Beijing 100730, China
[2]Department of Orthopedic Surgery, First Hospital of Harbin, Harbin 150010, China
[3]Department of Orthopedic Surgery, Beijing Tongren Hospital, Capital Medical University, Beijing 100730, China
*Equal contribution

Correspondence to: Xisheng Weng; **email:** xshweng@medmail.com.cn
Keywords: synoviocytes, RA, Mst1, AMPK, Sirt1
Received: February 19, 2020 **Accepted:** June 19, 2020 **Published:** July 21, 2020

ABSTRACT

In this study, we investigated the role of macrophage stimulating 1 (Mst1) and the AMPK-Sirt1 signaling pathway in the oxidative stress-induced mitochondrial dysfunction and apoptosis seen in rheumatoid arthritis-related fibroblast-like synoviocytes (RA-FLSs). Mst1 mRNA and protein expression was significantly higher in hydrogen peroxide (H_2O_2)-treated RA-FLSs than untreated controls. H_2O_2 treatment induced the mitochondrial apoptotic pathway by activating caspase3/9 and Bax in the RA-FLSs. Moreover, H_2O_2 treatment significantly reduced mitochondrial membrane potential and mitochondrial state-3 and state-4 respiration, but increased reactive oxygen species (ROS). Mst1 silencing significantly reduced oxidative stress-induced mitochondrial dysfunction and apoptosis in RA-FLSs. Sirt1 expression was significantly reduced in the H_2O_2-treated RA-FLSs, but was higher in the H_2O_2-treated Mst1-silenced RA-FLSs. Pretreatment with selisistat (Sirt1-specific inhibitor) or compound C (AMPK antagonist) significantly reduced the viability and mitochondrial function in H_2O_2-treated Mst1-silenced RA-FLSs by inhibiting Sirt1 function or Sirt1 expression, respectively. These findings demonstrate that oxidative stress-related upregulation and activation of Mst1 promotes mitochondrial dysfunction and apoptosis in RA-FLSs by inhibiting the AMPK-Sirt1 signaling pathway. This suggests the Mst1-AMPK-Sirt1 axis is a potential target for RA therapy.

INTRODUCTION

Rheumatoid arthritis (RA) is a chronic and progressive systemic autoimmune disease that affects bones and joints [1]. The pathogenesis of RA involves infiltration of inflammatory cells into the joints, degeneration of the synoviocytes and abnormal synovial hyperplasia caused by infiltration of the fibroblast-like synoviocytes (FLSs) that eventually leads to destruction of the cartilage and bone [2]. Anti-inflammatory and immunomodulatory drugs are the primary modes of treating RA [3].

Oxidative stress-induced cellular apoptosis plays an integral role in RA pathogenesis [4]. Excessive ROS production and metabolic alterations promote senescence of the synoviocytes as well as excessive proliferation of the fibroblasts [5]. Moderate activation of the fibroblasts promote regeneration of the synoviocytes by producing paracrine cell growth factors such as vascular endothelial growth factor (VEGF), fibroblast growth factor (FGF) and platelet derived growth factor (PDGF), whereas, uncontrolled oxidative stress promotes phenotypic changes in the fibroblasts, thereby resulting in collagen deposition and subchondral bone erosion [6]. Chronic oxidative stress also triggers synoviocyte cell death causing loss of bone tissue and fibrosis [7]. Therefore, reducing

oxidative stress and synoviocyte apoptosis is critical for suppressing RA development and progression.

Macrophage stimulating 1 (Mst1) is a protein kinase that promotes apoptosis through phosphorylation of Forkhead box O (FOXO) transcription factors [8]. Mst1 is part of the Hippo signaling pathway, which controls cellular proliferation and tissue growth. Mst1 activation is associated with oxidative stress-induced cellular apoptosis in cardiomyocytes [9] and endothelial cells [10]. During cardiac ischemia reperfusion injury, Mst1 interacts with Bcl2 and activates the Bax-mediated mitochondrial pathway of apoptosis [11]. In acute cerebral damage, Mst1 inhibits MAPK-ERK signaling pathway, thereby suppressing the expression of anti-apoptotic genes [12]. During inflammatory response, Mst1 induces apoptosis by reducing mitochondrial membrane potential through phosphorylation of c-Jun N-terminal kinase [13].

Sirtuin 1 (Sirt1) is a NAD^+-dependent histone/protein deacetylase that regulates cellular metabolism, senescence or aging, survival, stress resistance, and oxidative stress [14]. Sirt1 induces the expression of several antioxidant proteins, such as GSH, SOD, and GPX [15]. Sirt1 also inhibits oxidative stress-related signaling pathways, such as NF-κB or JNK. Sirt1 overexpression reduces the oxidative stress-induced apoptosis in the cartilage tissue by modulating BMP2 activity [16]. Moreover, Sirt1 regulates Mst1/YAP2 activation in hepatocellular carcinoma cells, thereby modulating tumor growth and progression [17]. In this study, we investigated the relationship between Sirt1 and Mst1 in oxidative stress-induced synoviocyte apoptosis with implications for RA therapy.

RESULTS

Mst1 mediates oxidative stress-induced caspase-3 dependent apoptosis in the RA-FLSs

We induced oxidative stress in RA-FLSs using hydrogen peroxide (H_2O_2) and analyzed its effects on Mst1 expression. QRT-PCR analysis demonstrated that Mst1 mRNA levels were significantly higher in the H_2O_2-treated RA-FLSs compared to the untreated controls (Figure 1A). Furthermore, immunofluorescence assays showed that Mst1 protein levels were significantly upregulated in the H_2O_2-treated RA-FLSs compared to the untreated controls (Figure 1B, 1C). These results demonstrate that oxidative stress upregulates Mst1 expression in the RA-FLSs.

Next, we knocked down Mst1 in RA-FLSs using Mst1-specific shRNA (sh-Mst1) and investigated the oxidative stress response of Mst1-silenced RA-FLSs. MTT assay results demonstrated that the viability of H_2O_2-treated Mst1-silenced RA-FLSs was significantly higher compared to the viability of H_2O_2-treated RA-FLSs (Figure 1D). Furthermore, ELISA assays showed that caspase-3 activity was significantly lower in the H_2O_2-treated Mst1-silenced RA-FLSs compared to the H_2O_2-treated RA-FLSs (Figure 1E). TUNEL assay showed that apoptotic rate of H_2O_2-treated RA-FLSs was significantly higher compared to untreated controls and H_2O_2-treated Mst1-silenced RA-FLSs (Tunel-positive cells: 38% vs. 3% vs. 10%; Figure 1F–1G). This suggests that Mst1 mediates oxidative stress-induced apoptosis in the RA-FLSs.

Mst1 activation induces mitochondrial dysfunction in oxidative stress-induced RA-FLSs

Mitochondria play a significant role in the regulation of cellular apoptosis and oxidative stress [18, 19]. Therefore, we investigated if Mst1 promotes apoptosis in H_2O_2-treated RA-FLSs by triggering mitochondrial dysfunction. Mitochondrial membrane potential was significantly reduced in the H_2O_2-treated RA-FLSs compared to untreated controls and H_2O_2-treated Mst1 knockdown RA-FLSs based on JC-1 staining (Figure 2A, 2B). ELISA assay showed that state-3 and state-4 mitochondrial respiration was significantly decreased in the H_2O_2-treated RA-FLSs compared to the untreated controls, but remained higher in the H_2O_2-treated Mst1 knockdown RA-FLSs (Figure 2C, 2D). ROS levels were significantly higher in the H_2O_2-treated RA-FLSs compared to the untreated controls, but lower in the H_2O_2-treated Mst1 knockdown RA-FLSs based on DCFDA staining (Figure 2E, 2F). These results suggest that oxidative stress induces mitochondrial dysfunction by activating Mst1.

Finally, we analyzed the status of the mitochondrial apoptotic pathway using ELISA assays. Caspase-9 and Bax activities were significantly increased in the H_2O_2-treated RA-FLSs compared to the untreated controls, but were significantly lower in the H_2O_2-treated Mst1 knockdown RA-FLSs (Figure 2G, 2H). This suggests that Mst1 promotes oxidative stress-mediated mitochondrial apoptosis in RA-FLSs.

Mst1 inhibits Sirt1 expression in oxidative stress-induced RA-FLSs

Next, we explored the downstream effectors of Mst1 that regulate mitochondrial dysfunction and apoptosis in RA-FLSs. Towards this, we investigated the functional status of Sirt1, which has been previously reported to be associated with cartilage apoptosis [16]. QRT-PCR analysis showed that Sirt1 mRNA levels were significantly reduced in H_2O_2-treated RA-FLSs com-

pared to the untreated controls, but remained higher in the H_2O_2-treated Mst1 knockdown RA-FLSs (Figure 3A). Immunofluorescence assays showed that Sirt1 protein levels were significantly reduced in the H_2O_2-treated RA-FLSs compared to the untreated controls, but were higher in the H_2O_2-treated Mst1 knockdown RA-FLSs (Figure 3B, 3C). We then measured the mRNA expression of Sirt3 and Sirt6, the other members of the Sirtuin family, and observed that Sirt3 and Sirt6 levels were downregulated in the H_2O_2-treated RA-FLSs as well as H_2O_2-treated Mst1 knockdown RA-FLSs compared to the untreated controls (Figure 3D, 3E).

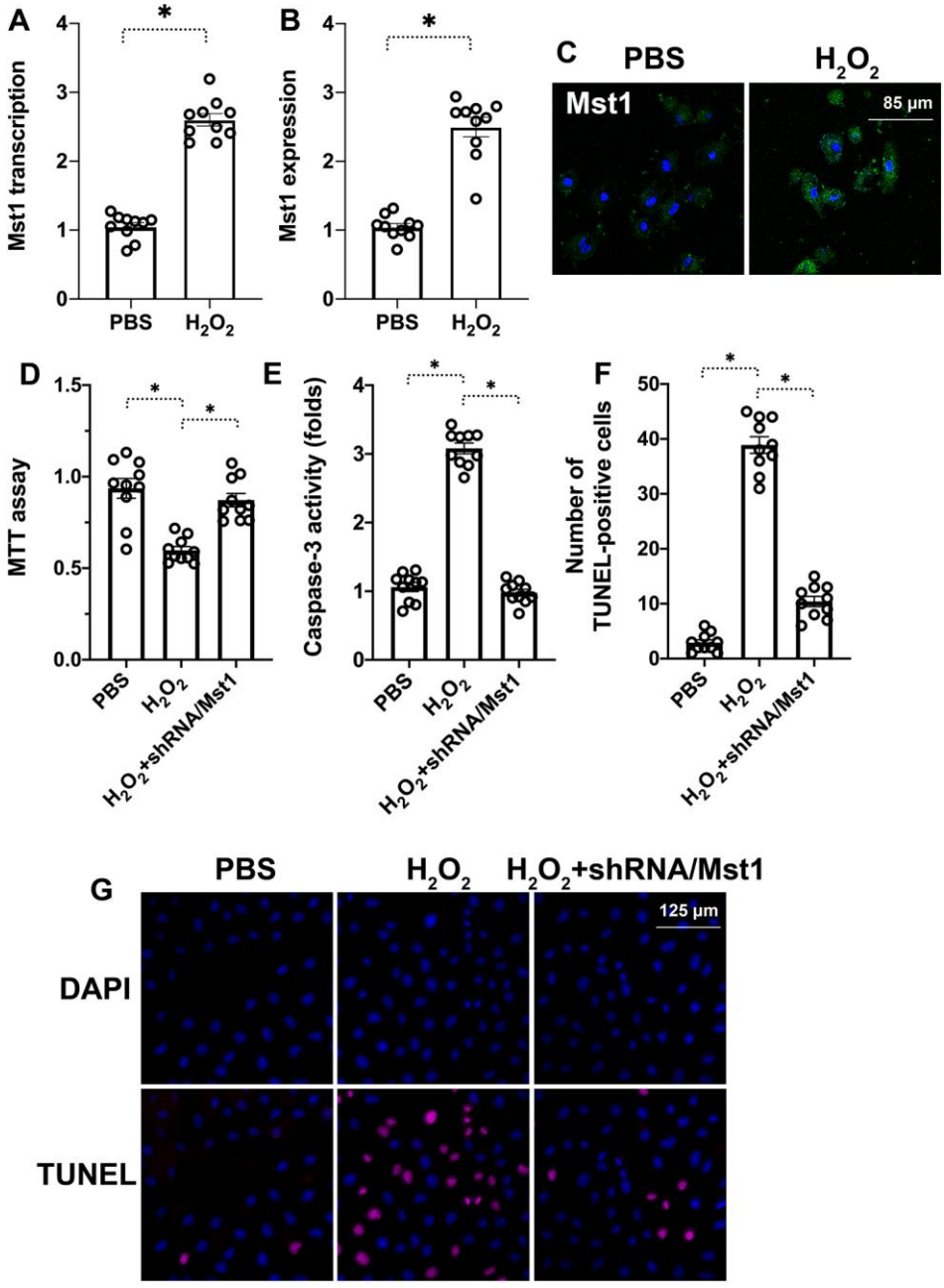

Figure 1. Mst1 promotes apoptosis in oxidative stress-induced RA-FLSs. (**A**) QRT-PCR analysis shows Mst1 mRNA levels in the control and H_2O_2-treated RA-FLSs. (**B**) Representative immunofluorescence images show Mst1 protein expression in control and H_2O_2-treated RA-FLSs (**C**) Quantitative estimation of relative Mst1 protein levels in control and H_2O_2-treated RA-FLSs based on the immunofluorescence assay. (**D**) MTT assay results show the viability of control and Mst1 knockdown RA-FLSs treated with or without H_2O_2. (**E**) ELISA assay results show caspase-3 activity in the control and H_2O_2-treated RA-FLSs. (**F**) Representative images show TUNEL staining of the control and H_2O_2-treated RA-FLSs. (**G**) Quantification of percent TUNEL-positive (apoptotic) cells in the control and H_2O_2-treated RA-FLSs. Note: RA-FLSs were treated with 0.3 mM H_2O_2 for 6 h; *P<0.05.

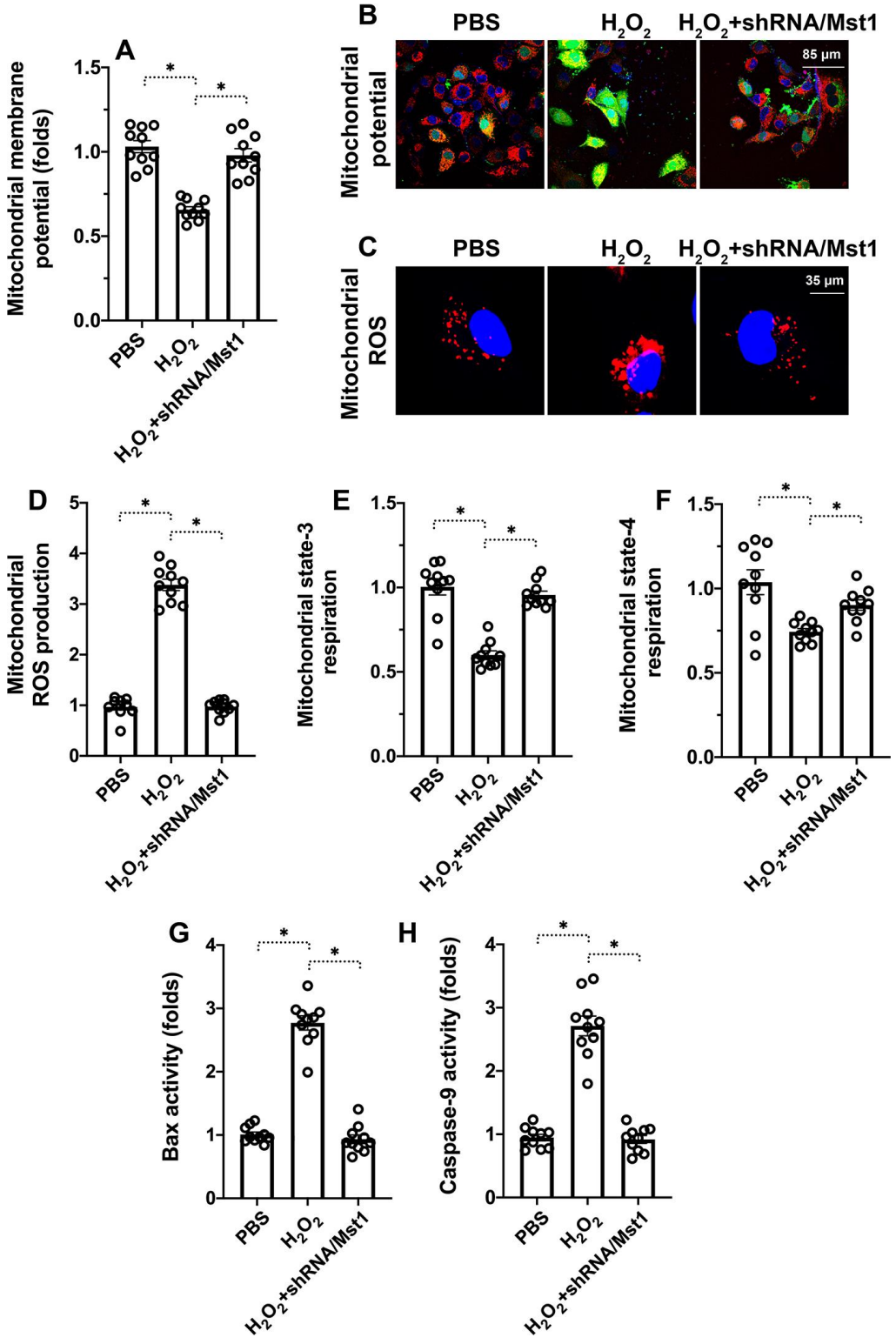

Figure 2. Mst1 induces mitochondrial dysfunction in oxidative stress-induced RA-FLSs. (**A**, **B**) Representative images show JC-1 staining to determine mitochondrial membrane potential in control and H_2O_2-treated RA-FLSs. Mitochondrial potential was measured by the ratio of red-to-green JC-1 fluorescence intensity. (**C**, **D**) ELISA assay results show mitochondrial state-3 and state-4 respiration rates in the control and H_2O_2-treated RA-FLSs. (**E**, **F**) Representative fluorescence microscopic images show DCFDA staining to determine ROS levels in the control and Mst1-silenced RA-FLSs treated with or without H_2O_2. ROS levels were quantified based on the DCFDA staining intensities. (**G**–**H**) ELISA assay results show caspase-9 and Bax activities in the control and H_2O_2-treated RA-FLSs. Note: RA-FLSs were treated with 0.3 mM H_2O_2 for 6 h; *P<0.05.

Taken together, our results confirm that Mst1 specifically inhibits Sirt1 expression in oxidative stress-induced RA-FLSs.

Sirt1 regulates survival and mitochondrial function in Mst1-knockdown RA-FLSs

Next, we analyzed if reduced Sirt1 expression was responsible for apoptosis and mitochondrial dysfunction in H_2O_2-treated RA-FLSs. We used selisistat, a potent inhibitor of Sirt1 to suppress its inhibited Sirt1 in H_2O_2-treated Mst1 knockdown RA-FLSs using selisistat, a potent inhibitor of Sirt1, and analyzed its effects through biochemical assays. MTT assay results showed that H_2O_2 treatment significantly reduced the viability of selisistat-pretreated Mst1-knockdown RA-FLSs compared to the control Mst1-knockdown RA-FLSs (Figure 4A). Tunel assay showed that the numbers of apoptotic (Tunel-positive) cells were significantly higher in the selisistat-pretreated Mst1-knockdown RA-FLSs compared to the control Mst1-knockdown RA-FLSs when treated with H_2O_2 (Figure 4B, 4C). Furthermore, mitochondrial membrane potential was significantly reduced (Figure 4D, 4E) and ROS levels were significantly higher (Figure 4F, 4G) in the selisistat-pretreated Mst1-knockdown RA-FLSs compared to the control Mst1-knockdown RA-FLSs upon H_2O_2 treatment. These results demonstrate that Sirt1 is required for survival and mitochondrial function in oxidative stress-induced Mst1-knockdown RA-FLSs.

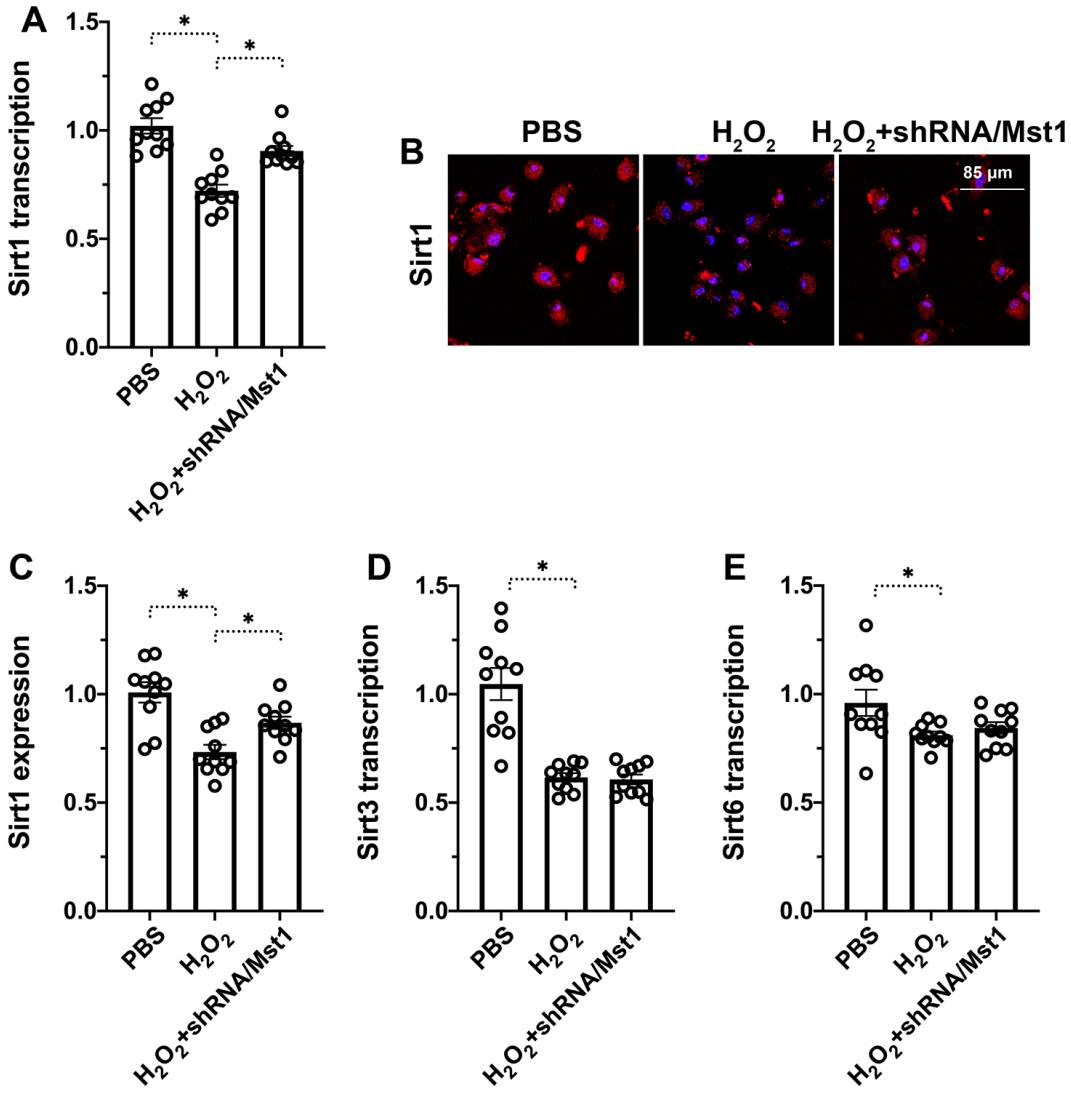

Figure 3. Mst1-dependent Sirt1 downregulation in oxidative stress-induced RA-FLSs. (**A**) QRT-PCR assay shows Sirt1 mRNA levels in control and H_2O_2-treated RA-FLSs. (**B**, **C**) Immunofluorescence staining shows Sirt1 protein levels in the control and Mst1-silenced RA-FLSs treated with or without H_2O_2. (**D**, **E**) QRT-PCR assay shows Sirt3 and Sirt6 mRNA levels in the control and H_2O_2-treated RA-FLSs. Note: RA-FLSs were treated with 0.3 mM H_2O_2 for 6 h; *P<0.05.

Mst1 reduces Sirt1 expression through inhibiting AMPK pathway

Finally, we investigated the role of AMPK signaling pathway, a key regulator of Sirt1 stability and function, in the survival of oxidative stress-induced Mst1-knockdown RA-FLSs by using compound C (CC), the inhibitor of AMPK. QRT-PCR analysis showed that Sirt1 mRNA levels were significantly reduced in compound C-pretreated Mst1-knockdown RA-FLSs compared to the Mst1-knockdown RA-FLSs, when treated with H_2O_2 (Figure 5A). Immunofluorescence assays showed that Sirt1 protein levels were significantly lower in the compound C-pretreated Mst1-knockdown RA-FLSs compared to the Mst1-knockdown RA-FLSs, when treated with H_2O_2 (Figure 5B, 5C). QRT-PCR analysis

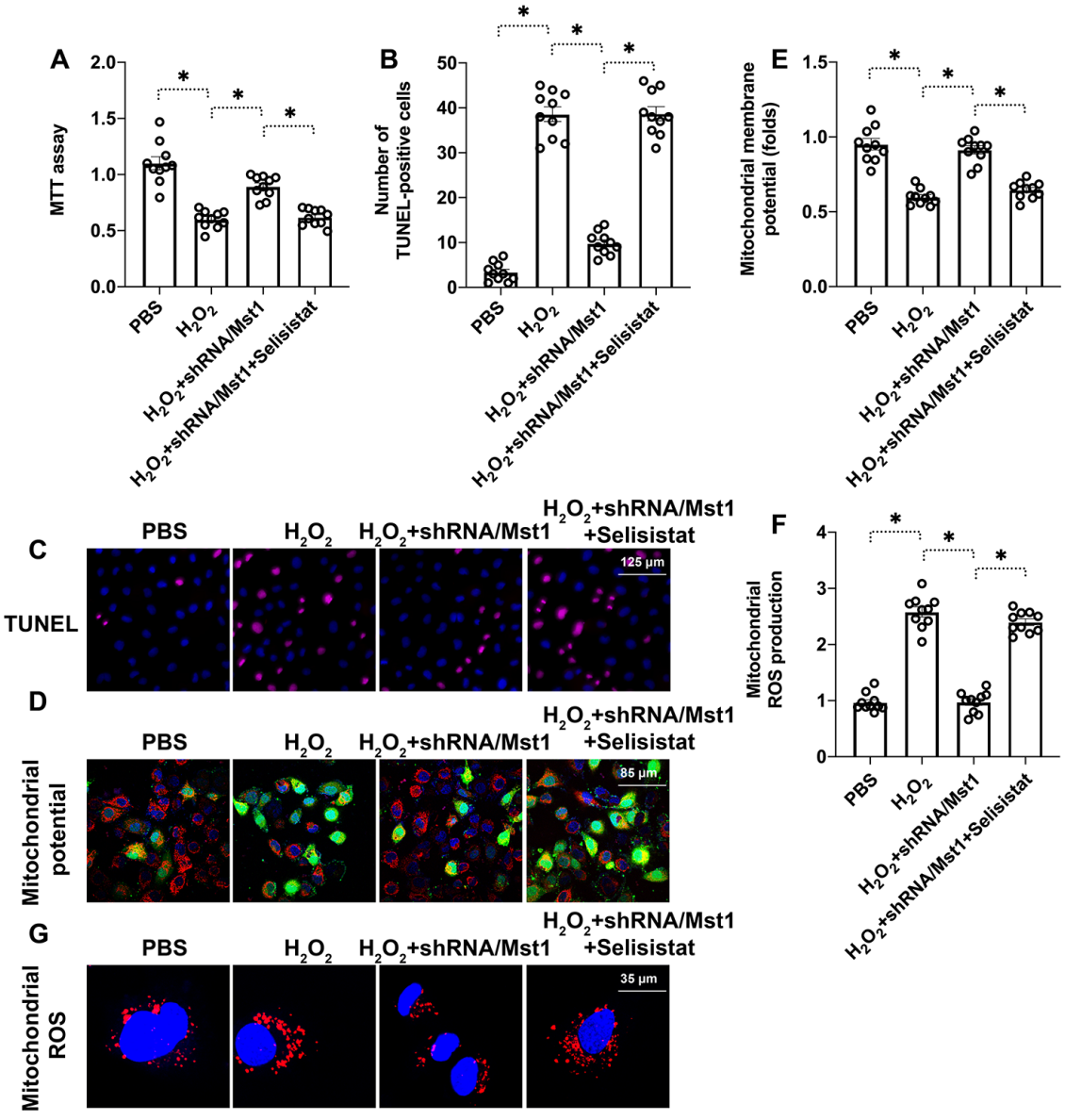

Figure 4. Sirt1 inhibition abolishes the beneficial effects of Mst1 knockdown in oxidative stress-induced RAFLSs. (**A**) MTT assay results show the viability of control and Mst1-knockdown RA-FLSs, pretreated with or without selisistat, a potent inhibitor of Sirt1. (**B**, **C**) TUNEL assay results show the apoptotic rates (percent Tunel-positive cells) in the control and Mst1-knockdown RA-FLSs, pretreated with or without selisistat, and treated with or without 0.3 mM H_2O_2 for 6 h. (**D**, **E**) JC-1 staining assay results show mitochondrial membrane in the control and Mst1-knockdown RA-FLSs, pretreated with or without selisistat, and treated with or without 0.3 mM H_2O_2 for 6 h. Mitochondrial potential was measured by the ratio of red-to-green JC-1 fluorescence intensity. (**F**–**G**) Representative fluorescence microscopic images show the DCFDA staining to determine ROS levels in the control and Mst1-knockdown RA-FLSs, pretreated with or without selisistat, and treated with or without 0.3 mM H_2O_2 for 6 h. ROS levels were quantified based on DCFDA staining intensity. *P<0.05.

also showed that H_2O_2treatment increased Sirt3 and Sirt6 levels in Mst1-knockdown RA-FLSs with or without compound pre-treatment (Figure 5D, 5E). These data demonstrate that Mst1 specifically inhibits Sirt1 expression through the AMPK pathway in the oxidative stress-induced RA-FLSs.

DISCUSSION

In the present study, we demonstrate that oxidative stress-induced apoptosis and mitochondrial dysfunction in the synoviocytes is associated with increased Mst1 expression and dysregulated AMPK-Sirt1 signaling pathway. Oxidative stress upregulates Mst1 expression in the synoviocytes. Mst1 decreases mitochondrial respiration and mitochondrial membrane potential and increases ROS levels by suppressing AMPK-Sirt1 signaling pathway. Subsequently, Mst1 upregulation promotes Bax- and caspase-3/9-dependent mitochondrial apoptosis in oxidative stress-induced synoviocytes. Therefore, our study demonstrates that Mst1- AMPK-Sirt1 axis is a novel therapeutic target to alleviate oxidative damage-related dysfunction of the synoviocytes in RA patients.

RA is a disease caused by chronic inflammation involving recruitment of pro-inflammatory immune cells, oxidative stress and synoviocyte apoptosis, collagen accumulation and bone tissue degradation [20–23]. Therapeutic strategies that reduce free radical generation and oxidative damage relieve common symptoms such as pain and stiffness in RA patients. Drugs that reduce oxidative stress and pro-inflammatory cytokine levels, such as, Rhoifolin [24], rosmarinic acid [25], and alogliptin [26] have

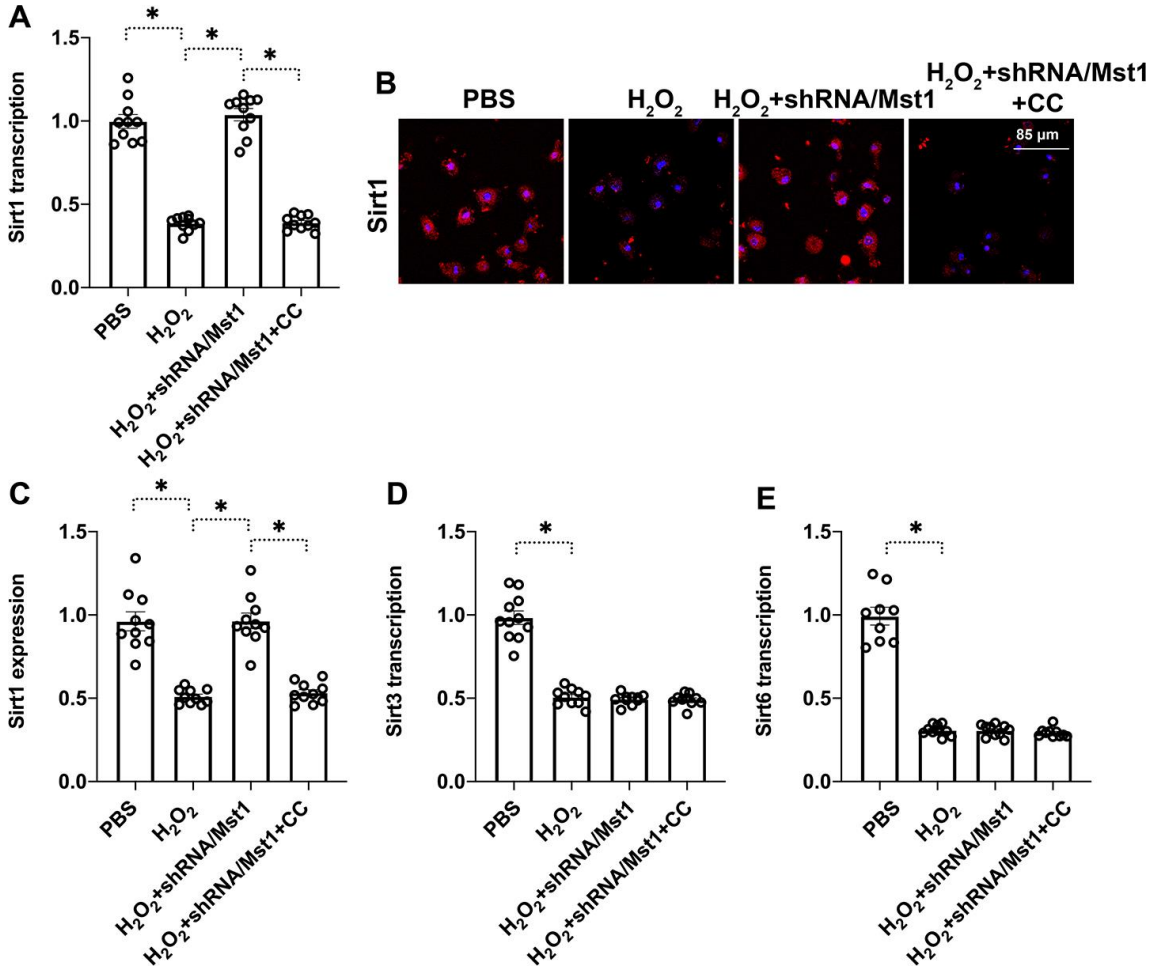

Figure 5. Mst1 reduces Sirt1 expression in oxidative stress-induced RA-FLSs by inhibiting the AMPK signaling pathway. (**A**) QRT-PCR assay results show the Sirt1 mRNA levels in the control and Mst1-knockdown RA-FLSs, pretreated with or without compound C, and treated with or without 0.3 mM H_2O_2 for 6 h. Compound C (CC) is an antagonist of the AMPK pathway. (**B**, **C**) Immunofluorescence staining results show Sirt1 protein levels in the control and Mst1-knockdown RA-FLSs, pretreated with or without compound C, and treated with or without 0.3 mM H_2O_2 for 6 h. (**D**, **E**) QRT-PCR analysis shows Sirt3 and Sirt6 mRNA levels in the control and Mst1-knockdown RA-FLSs, pretreated with or without compound C, and treated with or without 0.3 mM H_2O_2 for 6 h. *P<0.05.

commonly been used for RA therapy. However, the molecular mechanisms underlying oxidative stress-mediated dysfunction and death of synoviocytes are not clear. Our study demonstrates that oxidative stress increases Mst1 expression in the synoviocytes. Mst1 is a pro-apoptotic protein that was first described in studies related to HCC progression [27]. Subsequently, Mst1 has been implicated in pathology related to cerebral ischemia-reperfusion injury [12, 28], septic cardiomyopathy [13, 29], atherosclerosis [30], neuroinflammation [31], and diabetes-related microvascular dysfunction [32]. Mst1 upregulation is associated with increased ROS and decreased ATP levels that subsequently cause cellular apoptosis [33, 34]. Thus, our study implies that Mst1 is a potential target for RA therapy.

Sirt1 is a critical component of the mitochondrial quality control machinery and is involved in the regulation of mitochondrial biogenesis, mitochondrial oxidative stress, and mitochondrial dynamics [35–37]. A recent study by Leblond et al. showed that Sirt1 is associated with synovial angiogenesis, which is critical pathological phenotype observed in RA patients [38]. Besides, Sirt1 modulates osteogenic differentiation by regulating the expression of retinoic acid receptors [39]. In RA, the proliferation of synovial fibroblasts and production of pro-inflammatory cytokines is partly inhibited by the miR-22/Sirt1 signaling pathway [40]. In the present study, we found that Sirt1 expression is significantly downregulated under oxidative stress in an Mst-dependent manner. However, Sirt1 expression is high in oxidative stress-induced Mst1-silenced synoviocytes and correlated with improved mitochondrial function and viability. However, Sirt1 inhibition or AMPK inhibition abolishes the beneficial effects of the Mst1 knockdown in the oxidative stress-induced synoviocytes. Therefore, our results demonstrate a causal relationship between Mst1 activation and Sirt1 downregulation in the oxidative stress-induced synoviocytes.

In conclusion, our study demonstrates that oxidative stress-induced Mst1 upregulation in the synoviocytes promotes mitochondrial dysfunction and apoptosis by inhibiting the AMPK-Sirt1 signaling pathway. Therefore, Mst1-AMPK-Sirt1 axis is a potential target for RA therapy.

MATERIALS AND METHODS

RA synoviocytes and cell culture

The human rheumatoid arthritis fibroblast-like synoviocytes (RA-FLSs; C0495) were obtained from Guandao Bioengineering Co., Ltd (Shanghai, China) and maintained in DMEM medium containing 10% FBS and 1% penicillin/streptomycin. The RA-FLSs were treated with 0.3 mM hydrogen peroxide for 6 h to induce oxidative stress as previously described [41–42]. The RA-FLSs were pre-treated for 4 h with selisistat, a potent inhibitor of Sirt1, to inhibit Sirt1 activity.

Construction of Mst1-shRNA recombinant lentivirus

Lentivirus particles containing Mst1 shRNA were prepared as previously described [43]. Briefly, the shRNA against Mst1 was inserted into the pBS-SKII-hU6 vector downstream of the hU6 promoter [44]. The shRNA expression cassette was then confirmed by DNA sequencing. Lentiviral stocks were prepared by Polyetherimide (PEI) co-transfecting HEK293T cells with the lentiviral expression and packaging plasmids, psPAX2 and pMD2.G. The supernatants were collected at 48 h and 72 h after transfection [45], and the lentiviral particles were concentrated using a 0.45 μm filter (Millipore Corp, Billerica, MA, USA). The recombinant lentiviruses were used to infect RA-FLSs using 4 μg/ml polybrene.

Western blotting

The cells were lysed with the RIPA buffer for 2 h on ice and centrifuged at 13,200 rpm for 15 min at 4°C. The protein concentration in the supernatant was determined using the Bio-Rad protein assay kit (Bio-Rad, Hercules, CA, USA) according to the manufacturer's protocol [46]. Equal amounts of total cellular protein lysates were subjected to SDS–PAGE electrophoresis, transferred to pre-activated polyvinylidene fluoride membranes (Millipore Corp, Billerica, MA, USA), and the membranes were blocked with 5% skimmed milk in TBST at room temperature for 1 h [47]. The membranes were then incubated overnight at 4°C with primary antibodies against Mst1, Sirt1 and GAPDH (Santa Cruz Biotechnology). Then, the blots were incubated with HRP-conjugated secondary antibodies at room temperature for 1 h. The blots were developed using Enhanced Chemiluminescence (ECL) solution and visualized [48]. The protein bands were quantified using the Image J software and relative amounts of proteins were estimated using GAPDH as the internal control [49].

Immunofluorescence staining

For immunofluorescence staining, the cells were fixed with 3.7% formaldehyde in PBS and blocked with 0.1% BSA solution. The slides were then incubated overnight at 4°C with primary antibodies [50]. Then, after rinsing with PBS, the slides were incubated with Alexa Fluor® 488 goat anti-mouse and Alexa Fluor® 594 goat anti-rat secondary antibodies (Thermo

Fischer, Waltham, MA) [51]. The nuclei were stained with DAPI. The stained cells were visualized under a Zeiss LSM 700 confocal laser scanning microscope (Carl Zeiss, Germany) with a 63x oil immersion objective using a dual filter set for DAPI and FITC or rhodamine. The images were captured using the ZEN software (Carl Zeiss, Germany) [52].

TUNEL

TUNEL was performed using the *In situ* cell death detection kit (Roche, Shanghai, China) as previously described [53]. Briefly, the sections were fixed with 4% paraformaldehyde, permeabilized with buffer containing 0.5% Triton X-100 and 0.05% SDS, and then incubated with TUNEL reaction mixture in the reaction buffer [54]. The nuclei were stained with DAPI and then the specimens were visualized under microscope. TUNEL-positive cells were counted in five fields at 200x magnification for each slide and normalized to DAPI staining numbers using the Image J software [55].

Enzyme-linked immunosorbent assay (ELISA)

For the ELISA assays, we used 2 mg of the whole cell lysate in 100 µl buffer to detect intracellular proteins, whereas for secreted proteins, 20 ml of the culture medium was concentrated using the 3 kDa cut-off Amicon Ultra-15 Centrifugal Filter (#UFC900308, EMD Millipore) to detect the concentration of targeted proteins. ELISA assays were performed according to the manufacturer's instructions [56].

ROS detection

The DCFDA Cellular Reactive Oxygen Species Detection Assay Kit (ab113851; Abcam) was used to estimate the reactive oxygen species (ROS) levels in cells [57]. Briefly, 2.5 x 10^4 cells per well were seeded in dark, clear bottom 96-well microplates and allowed to adhere overnight. Then, the cells were incubated with 25 µM DCFDA for 1 h at 37°C. The fluorescence was analyzed using a fluorescent plate reader at an excitation wavelength at 485 nm and an emission wavelength at 535 nm [58].

Quantitative real time PCR (qPCR)

Total cellular RNA was isolated using the RNeasy mini Kit (Qiagen, Hilden, Germany), purity and quantified using the Nanodrop spectrophotometer (Thermo Scientific, Waltham, MA). Then, cDNA was synthesized using MultiScribe reverse transcriptase, random primers, deoxyribose nucleoside triphosphate (dNTP) mix and RNase inhibitor (all Applied Biosystems, Foster City, CA) in a Quanta Biotech Q Cycler II according to the following cycling conditions: 2 min at 50°C; 10 min at 95°C; 40 cycles of 15 seconds at 95°C and 60 seconds at 60°C. Then, qPCR was performed using Taqman gene assays [59]. Relative gene expression was analyzed using the $2^{-\Delta\Delta Ct}$ method with GAPDH as the internal control.

Statistical analysis

The data are presented as the means ± standard deviation (SD). All biochemical analyses were performed at least in triplicate. The differences between multiple groups were analyzed using one-way analysis of variance (ANOVA) and the differences between two groups were analyzed using the 2-tailed Student's t-test, followed by Dunnett's and Tukey's tests. $P < 0.05$ was considered statistically significant. Pearson's correlation coefficients were calculated to evaluate the association between clinical parameters. All statistical analyses were performed using the GraphPad Prism version 5.0 for Windows (GraphPad Software, San Diego, CA, USA).

CONFLICTS OF INTEREST

The authors declare that there are no conflicts of interest.

REFERENCES

1. Engin B, Sevim A, Cesur SK, Tüzün Y. Eruptions in life-threatening rheumatologic diseases. Clin Dermatol. 2020; 38:86–93. https://doi.org/10.1016/j.clindermatol.2019.10.016 PMID:32197752

2. Tanaka S, Hammond B, Rosin DL, Okusa MD. Neuroimmunomodulation of tissue injury and disease: an expanding view of the inflammatory reflex pathway. Bioelectron Med. 2019; 5:13. https://doi.org/10.1186/s42234-019-0029-8 PMID:32232102

3. Somers EC. Pregnancy and autoimmune diseases. Best Pract Res Clin Obstet Gynaecol. 2020; 64:3–10. https://doi.org/10.1016/j.bpobgyn.2019.11.004 PMID:32173263

4. da Fonseca LJ, Nunes-Souza V, Goulart MO, Rabelo LA. Oxidative stress in rheumatoid arthritis: what the future might hold regarding novel biomarkers and add-on therapies. Oxid Med Cell Longev. 2019; 2019:7536805. https://doi.org/10.1155/2019/7536805 PMID:31934269

5. Souliotis VL, Vlachogiannis NI, Pappa M, Argyriou A, Ntouros PA, Sfikakis PP. DNA damage response and

oxidative stress in systemic autoimmunity. Int J Mol Sci. 2019; 21:55.
https://doi.org/10.3390/ijms21010055
PMID:31861764

6. Khan H, Sureda A, Belwal T, Çetinkaya S, Süntar İ, Tejada S, Devkota HP, Ullah H, Aschner M. Polyphenols in the treatment of autoimmune diseases. Autoimmun Rev. 2019; 18:647–57.
https://doi.org/10.1016/j.autrev.2019.05.001
PMID:31059841

7. Cecchi I, Arias de la Rosa I, Menegatti E, Roccatello D, Collantes-Estevez E, Lopez-Pedrera C, Barbarroja N. Neutrophils: novel key players in rheumatoid arthritis. Current and future therapeutic targets. Autoimmun Rev. 2018; 17:1138–49.
https://doi.org/10.1016/j.autrev.2018.06.006
PMID:30217550

8. Yamaguchi Y, Madhyastha H, Madhyastha R, Choijookhuu N, Hishikawa Y, Pengjam Y, Nakajima Y, Maruyama M. Arsenic acid inhibits proliferation of skin fibroblasts, and increases cellular senescence through ROS mediated MST1-FOXO signaling pathway. J Toxicol Sci. 2016; 41:105–13.
https://doi.org/10.2131/jts.41.105
PMID:26763397

9. Lu K, Zhao J, Liu W. Macrophage stimulating 1-induced inflammation response promotes aortic aneurysm formation through triggering endothelial cells death and activating the NF-κB signaling pathway. J Recept Signal Transduct Res. 2020; 40:374–82.
https://doi.org/10.1080/10799893.2020.1738484
PMID:32156191

10. Zhang J, Zhang F. Suppressor of ras val-2 promotes inflammation-mediated oxidative stress and cell apoptosis in cardiomyocytes through activating Mst1-mROS signaling pathway. J Recept Signal Transduct Res. 2020; 40:224–30.
https://doi.org/10.1080/10799893.2020.1726953
PMID:32065019

11. Birnboim HC. Spacing of polypyrimidine regions in mouse DNA as determined by poly(adenylate, guanylate) binding. J Mol Biol. 1978; 121:541–59.
https://doi.org/10.1016/0022-2836(78)90399-6
PMID:671548

12. Zhou D, Zhang M, Min L, Jiang K, Jiang Y. Cerebral ischemia-reperfusion is modulated by macrophage-stimulating 1 through the MAPK-ERK signaling pathway. J Cell Physiol. 2020. [Epub ahead of print].
https://doi.org/10.1002/jcp.29603
PMID:32017081

13. Ouyang H, Li Q, Zhong J, Xia F, Zheng S, Lu J, Deng Y, Hu Y. Combination of melatonin and irisin ameliorates lipopolysaccharide-induced cardiac dysfunction through suppressing the Mst1-JNK pathways. J Cell Physiol. 2020. [Epub ahead of print].
https://doi.org/10.1002/jcp.29561
PMID:31976559

14. Singh V, Ubaid S. Role of silent information regulator 1 (SIRT1) in regulating oxidative stress and inflammation. Inflammation. 2020. [Epub ahead of print].
https://doi.org/10.1007/s10753-020-01242-9
PMID:32410071

15. Nagappan A, Kim JH, Jung DY, Jung MH. Cryptotanshinone from the Salvia miltiorrhiza bunge attenuates ethanol-induced liver injury by activation of AMPK/SIRT1 and Nrf2 signaling pathways. Int J Mol Sci. 2019; 21:265.
https://doi.org/10.3390/ijms21010265
PMID:31906014

16. Lu Y, Zhou L, Wang L, He S, Ren H, Zhou N, Hu Z. The role of SIRT1 in BMP2-induced chondrogenic differentiation and cartilage maintenance under oxidative stress. Aging (Albany NY). 2020; 12:9000–13.
https://doi.org/10.18632/aging.103161
PMID:32445555

17. Mao B, Hu F, Cheng J, Wang P, Xu M, Yuan F, Meng S, Wang Y, Yuan Z, Bi W. SIRT1 regulates YAP2-mediated cell proliferation and chemoresistance in hepatocellular carcinoma. Oncogene. 2014; 33:1468–74.
https://doi.org/10.1038/onc.2013.88
PMID:23542177

18. Zhou H, Li D, Zhu P, Ma Q, Toan S, Wang J, Hu S, Chen Y, Zhang Y. Inhibitory effect of melatonin on necroptosis via repressing the Ripk3-PGAM5-CypD-mPTP pathway attenuates cardiac microvascular ischemia-reperfusion injury. J Pineal Res. 2018; 65:e12503.
https://doi.org/10.1111/jpi.12503
PMID:29770487

19. Zhou H, Wang S, Hu S, Chen Y, Ren J. ER-mitochondria microdomains in cardiac ischemia-reperfusion injury: a fresh perspective. Front Physiol. 2018; 9:755.
https://doi.org/10.3389/fphys.2018.00755
PMID:29962971

20. Chirathaworn C, Chansaenroj J, Poovorawan Y. Cytokines and chemokines in Chikungunya virus infection: protection or induction of pathology. Pathogens. 2020; 9:E415.
https://doi.org/10.3390/pathogens9060415
PMID:32471152

21. Fattah A, Asadi A, Shayesteh MR, Hesari FH, Jamalzehi S, Abbasi M, Mousavi MJ, Aslani S. Fertility and infertility implications in rheumatoid arthritis; state of the art. Inflamm Res. 2020; 69:721–29.

https://doi.org/10.1007/s00011-020-01362-w PMID:32458007

22. Shoor S. Risk of serious infection associated with agents that target t-cell activation and interleukin-17 and interleukin-23 cytokines. Infect Dis Clin North Am. 2020; 34:179–89. https://doi.org/10.1016/j.idc.2020.02.001 PMID:32444009

23. Lisitsyna TA, Ivanova MM, Durnev AD. [Active forms of oxygen and pathogenesis of rheumatoid arthritis and systemic lupus erythematosus]. Vestn Ross Akad Med Nauk. 1996; 15–20. PMID:9102073

24. Peng S, Hu C, Liu X, Lei L, He G, Xiong C, Wu W. Rhoifolin regulates oxidative stress and proinflammatory cytokine levels in freund's adjuvant-induced rheumatoid arthritis via inhibition of NF-κB. Braz J Med Biol Res. 2020; 53:e9489. https://doi.org/10.1590/1414-431x20209489 PMID:32401927

25. Sadeghi A, Bastin AR, Ghahremani H, Doustimotlagh AH. The effects of rosmarinic acid on oxidative stress parameters and inflammatory cytokines in lipopolysaccharide-induced peripheral blood mononuclear cells. Mol Biol Rep. 2020; 47:3557–66. https://doi.org/10.1007/s11033-020-05447-x PMID:32350743

26. Guo Q, Zhang S, Huang J, Liu K. Alogliptin inhibits IL-1β-induced inflammatory response in fibroblast-like synoviocytes. Int Immunopharmacol. 2020; 83:106372. https://doi.org/10.1016/j.intimp.2020.106372 PMID:32179246

27. Shi C, Cai Y, Li Y, Li Y, Hu N, Ma S, Hu S, Zhu P, Wang W, Zhou H. Yap promotes hepatocellular carcinoma metastasis and mobilization via governing cofilin/f-actin/lamellipodium axis by regulation of JNK/Bnip3/SERCA/CaMKII pathways. Redox Biol. 2018; 14:59–71. https://doi.org/10.1016/j.redox.2017.08.013 PMID:28869833

28. Sudrik CM, Cloutier T, Mody N, Sathish HA, Trout BL. Understanding the role of preferential exclusion of sugars and polyols from native state IgG1 monoclonal antibodies and its effect on aggregation and reversible self-association. Pharm Res. 2019; 36:109. https://doi.org/10.1007/s11095-019-2642-3 PMID:31127417

29. Yan T, Wang W, Yang L, Chen K, Chen R, Han Y. Rich club disturbances of the human connectome from subjective cognitive decline to Alzheimer's disease. Theranostics. 2018; 8:3237–55. https://doi.org/10.7150/thno.23772 PMID:29930726

30. Cao H, Jia Q, Yan L, Chen C, Xing S, Shen D. Quercetin suppresses the progression of atherosclerosis by regulating MST1-mediated autophagy in ox-LDL-induced RAW264.7 macrophage foam cells. Int J Mol Sci. 2019; 20:6093. https://doi.org/10.3390/ijms20236093 PMID:31816893

31. Zhou D, Jiang Y. Sirtuin 3 attenuates neuroinflammation-induced apoptosis in BV-2 microglia. Aging (Albany NY). 2019; 11:9075–89. https://doi.org/10.18632/aging.102375 PMID:31631063

32. Qin R, Lin D, Zhang L, Xiao F, Guo L. Mst1 deletion reduces hyperglycemia-mediated vascular dysfunction via attenuating mitochondrial fission and modulating the JNK signaling pathway. J Cell Physiol. 2020; 235:294–303. https://doi.org/10.1002/jcp.28969 PMID:31206688

33. Ma C, Fan L, Wang J, Hao L, He J. hippo/Mst1 overexpression induces mitochondrial death in head and neck squamous cell carcinoma via activating β-catenin/Drp1 pathway. Cell Stress Chaperones. 2019; 24:807–16. https://doi.org/10.1007/s12192-019-01008-9 PMID:31127452

34. Lu K, Liu X, Guo W. Melatonin attenuates inflammation-related venous endothelial cells apoptosis through modulating the MST1-MIEF1 pathway. J Cell Physiol. 2019; 234:23675–84. https://doi.org/10.1002/jcp.28935 PMID:31169304

35. Guan R, Cai Z, Wang J, Ding M, Li Z, Xu J, Li Y, Li J, Yao H, Liu W, Qian J, Deng B, Tang C, et al. Hydrogen sulfide attenuates mitochondrial dysfunction-induced cellular senescence and apoptosis in alveolar epithelial cells by upregulating sirtuin 1. Aging (Albany NY). 2019; 11:11844–64. https://doi.org/10.18632/aging.102454 PMID:31881011

36. Geng J, Wei M, Yuan X, Liu Z, Wang X, Zhang D, Luo L, Wu J, Guo W, Qin ZH. TIGAR regulates mitochondrial functions through SIRT1-PGC1α pathway and translocation of TIGAR into mitochondria in skeletal muscle. FASEB J. 2019; 33:6082–98. https://doi.org/10.1096/fj.201802209R PMID:30726106

37. Sim WC, Kim DG, Lee W, Sim H, Choi YJ, Lee BH. Activation of SIRT1 by l-serine increases fatty acid oxidation and reverses insulin resistance in C2C12 myotubes. Cell Biol Toxicol. 2019; 35:457–70. https://doi.org/10.1007/s10565-019-09463-x PMID:30721374

38. Leblond A, Pezet S, Cauvet A, Casas C, Pires Da Silva J, Hervé R, Clavel G, Dumas S, Cohen-Kaminsky S, Bessis N, Semerano L, Lemaire C, Allanore Y, Avouac J. Implication of the deacetylase sirtuin-1 on synovial angiogenesis and persistence of experimental arthritis. Ann Rheum Dis. 2020; 79:891–900. https://doi.org/10.1136/annrheumdis-2020-217377 PMID:32381568

39. Jung YJ, Park W, Noh JM, Kang KP, Nguyen-Thanh T, Han MK, Kim W. SIRT1 induces the adipogenic differentiation of mouse embryonic stem cells by regulating RA-induced RAR expression via NCOR1 acetylation. Stem Cell Res. 2020; 44:101771. https://doi.org/10.1016/j.scr.2020.101771 PMID:32217463

40. Zhang C, Fang L, Liu X, Nie T, Li R, Cui L, Wang J, Ji Y. miR-22 inhibits synovial fibroblasts proliferation and proinflammatory cytokine production in RASF via targeting SIRT1. Gene. 2020; 724:144144. https://doi.org/10.1016/j.gene.2019.144144 PMID:31629819

41. Zhang Y, Wang G, Wang T, Cao W, Zhang L, Chen X. Nrf2-Keap1 pathway-mediated effects of resveratrol on oxidative stress and apoptosis in hydrogen peroxide-treated rheumatoid arthritis fibroblast-like synoviocytes. Ann N Y Acad Sci. 2019; 1457:166–78. https://doi.org/10.1111/nyas.14196 PMID:31475364

42. Aanhane E, Schulkens IA, Heusschen R, Castricum K, Leffler H, Griffioen AW, Thijssen VL. Different angioregulatory activity of monovalent galectin-9 isoforms. Angiogenesis. 2018; 21:545–55. https://doi.org/10.1007/s10456-018-9607-8 PMID:29500586

43. Wider J, Undyala VV, Whittaker P, Woods J, Chen X, Przyklenk K. Remote ischemic preconditioning fails to reduce infarct size in the zucker fatty rat model of type-2 diabetes: role of defective humoral communication. Basic Res Cardiol. 2018; 113:16. https://doi.org/10.1007/s00395-018-0674-1 PMID:29524006

44. Aalto AL, Mohan AK, Schwintzer L, Kupka S, Kietz C, Walczak H, Broemer M, Meinander A. M1-linked ubiquitination by LUBEL is required for inflammatory responses to oral infection in drosophila. Cell Death Differ. 2019; 26:860–76. https://doi.org/10.1038/s41418-018-0164-x PMID:30026495

45. Gutierrez DA, DeJesus RE, Contreras L, Rodriguez-Palomares IA, Villanueva PJ, Balderrama KS, Monterroza L, Larragoity M, Varela-Ramirez A, Aguilera RJ. A new pyridazinone exhibits potent cytotoxicity on human cancer cells via apoptosis and poly-ubiquitinated protein accumulation. Cell Biol Toxicol. 2019; 35:503–19. https://doi.org/10.1007/s10565-019-09466-8 PMID:30825052

46. Amanakis G, Kleinbongard P, Heusch G, Skyschally A. Attenuation of ST-segment elevation after ischemic conditioning maneuvers reflects cardioprotection online. Basic Res Cardiol. 2019; 114:22. https://doi.org/10.1007/s00395-019-0732-3 PMID:30937537

47. Chrifi I, Louzao-Martinez L, Brandt MM, van Dijk CG, Bürgisser PE, Zhu C, Kros JM, Verhaar MC, Duncker DJ, Cheng C. CMTM4 regulates angiogenesis by promoting cell surface recycling of VE-cadherin to endothelial adherens junctions. Angiogenesis. 2019; 22:75–93. https://doi.org/10.1007/s10456-018-9638-1 PMID:30097810

48. Bommu UD, Konidala KK, Pamanji R, Yeguvapalli S. Computational screening, ensemble docking and pharmacophore analysis of potential gefitinib analogues against epidermal growth factor receptor. J Recept Signal Transduct Res. 2018; 38:48–60. https://doi.org/10.1080/10799893.2018.1426603 PMID:29369008

49. Chen Y, Liu K, Shi Y, Shao C. The tango of ROS and p53 in tissue stem cells. Cell Death Differ. 2018; 25:639–41. https://doi.org/10.1038/s41418-018-0062-2 PMID:29487352

50. Bramasole L, Sinha A, Gurevich S, Radzinski M, Klein Y, Panat N, Gefen E, Rinaldi T, Jimenez-Morales D, Johnson J, Krogan NJ, Reis N, Reichmann D, et al. Proteasome lid bridges mitochondrial stress with Cdc53/Cullin1 NEDDylation status. Redox Biol. 2019; 20:533–43. https://doi.org/10.1016/j.redox.2018.11.010 PMID:30508698

51. Chang L, Hu Y, Fu Y, Zhou T, You J, Du J, Zheng L, Cao J, Ying M, Dai X, Su D, He Q, Zhu H, Yang B. Targeting slug-mediated non-canonical activation of c-met to overcome chemo-resistance in metastatic ovarian cancer cells. Acta Pharm Sin B. 2019; 9:484–95. https://doi.org/10.1016/j.apsb.2019.03.001 PMID:31193822

52. Farber G, Parks MM, Lustgarten Guahmich N, Zhang Y, Monette S, Blanchard SC, Di Lorenzo A, Blobel CP. ADAM10 controls the differentiation of the coronary arterial endothelium. Angiogenesis. 2019; 22:237–50. https://doi.org/10.1007/s10456-018-9653-2 PMID:30446855

53. Liang P, Huang J. Off-target challenge for base editor-mediated genome editing. Cell Biol Toxicol. 2019; 35:185–87.

https://doi.org/10.1007/s10565-019-09474-8
PMID:31041571

54. Eid EE, Azam F, Hassan M, Taban IM, Halim MA. Zerumbone binding to estrogen receptors: an in-silico investigation. J Recept Signal Transduct Res. 2018; 38:342–51.
https://doi.org/10.1080/10799893.2018.1531886
PMID:30396310

55. Honda T, He Q, Wang F, Redington AN. Acute and chronic remote ischemic conditioning attenuate septic cardiomyopathy, improve cardiac output, protect systemic organs, and improve mortality in a lipopolysaccharide-induced sepsis model. Basic Res Cardiol. 2019; 114:15.
https://doi.org/10.1007/s00395-019-0724-3
PMID:30838474

56. Kim SY, Nair DM, Romero M, Serna VA, Koleske AJ, Woodruff TK, Kurita T. Transient inhibition of p53 homologs protects ovarian function from two distinct apoptotic pathways triggered by anticancer therapies. Cell Death Differ. 2019; 26:502–15.
https://doi.org/10.1038/s41418-018-0151-2
PMID:29988075

57. Moradi M, Najafi R, Amini R, Solgi R, Tanzadehpanah H, Esfahani AM, Saidijam M. Remarkable apoptotic pathway of hemiscorpius lepturus scorpion venom on CT26 cell line. Cell Biol Toxicol. 2019; 35:373–85.
https://doi.org/10.1007/s10565-018-09455-3
PMID:30617443

58. Motterlini R, Nikam A, Manin S, Ollivier A, Wilson JL, Djouadi S, Muchova L, Martens T, Rivard M, Foresti R. HYCO-3, a dual CO-releaser/Nrf2 activator, reduces tissue inflammation in mice challenged with lipopolysaccharide. Redox Biol. 2019; 20:334–48.
https://doi.org/10.1016/j.redox.2018.10.020
PMID:30391826

59. Park M, Sandner P, Krieg T. cGMP at the centre of attention: emerging strategies for activating the cardioprotective PKG pathway. Basic Res Cardiol. 2018; 113:24.
https://doi.org/10.1007/s00395-018-0679-9
PMID:29766323